REPORT DOCUMENTATION PAGE

Form Approved
OMB No. 0704-0188

1. REPORT DATE *(DD-MM-YYYY)*	**2. REPORT TYPE**	**3. DATES COVERED** *(From - To)*
May 2012	Technical Paper	May 2012-June 2012

4. TITLE AND SUBTITLE
NUMERICAL SIMULATION OF CONFINED MULTIPLE TRANSVERSE JETS

5a. CONTRACT NUMBER
In-House

5b. GRANT NUMBER

5c. PROGRAM ELEMENT NUMBER

6. AUTHOR(S)

F. Davoudzadeh, D. Forliti, A. Le, H. Vu

5d. PROJECT NUMBER

5e. TASK NUMBER

5f. WORK UNIT NUMBER
33SP0795

7. PERFORMING ORGANIZATION NAME(S) AND ADDRESS(ES)

Air Force Research Laboratory (AFMC)
AFRL/RQRE
4 Draco Drive.
Edwards AFB CA 93524-7160

8. PERFORMING ORGANIZATION REPORT NO.

9. SPONSORING / MONITORING AGENCY NAME(S) AND ADDRESS(ES)
Air Force Research Laboratory (AFMC)
AFRL/RQR
5 Pollux Drive
Edwards AFB CA 93524-7048

10. SPONSOR/MONITOR'S ACRONYM(S)

11. SPONSOR/MONITOR'S REPORT NUMBER(S)
AFRL-RZ-ED-TP-2012-201

12. DISTRIBUTION / AVAILABILITY STATEMENT
Distribution A: Approved for Public Release; Distribution Unlimited. PA#12436

13. SUPPLEMENTARY NOTES
Conference paper for the AIAA Fluid Dynamics Conference, New Orleans, LA, 25-28 June 2012.

14. ABSTRACT

Behavior of unconfined transverse jets has been studied extensively, but little work is reported on the flow characteristics of confined transverse jets. The latter has been numerically investigated using a number of RANS codes. The computational results obtained from these codes have been evaluated against the existing experimental data, and the results of a Large-Eddy Simulations (LES) code reported in the literature. Furthermore, an extensive validation effort has been conducted to characterize the performance of the codes for predicting the flow within a propulsion-related mixing configuration. The validation case involves eight circumferentially spaced transverse jets issuing radially into an axisymmetric main flow, a configuration relevant for gas turbine burners and new liquid rocket engine preburners. The main flow Reynolds number was 1.7 x 105 and the jet-to-main flow momentum flux ratio was sixteen. The momentum and scalar mixing was investigated through the solution of the Reynolds-Averaged Navier Stokes (RANS) equations. The solutions of three commercial RANS solvers, Fluent, STAR-CCM+, and CFD++, are compared to experimental data and large-eddy simulation (LES) results available in literature. Due to demonstrated periodicity, only a one-eighth pie-shaped section of the geometry was considered. The different commercial codes used the same geometry, grid, boundary conditions, and variations of the k-□ turbulence model. The LES results obtained from literature used a different grid, but the same geometry. All numerical simulations using the above mentioned codes capture salient flow structures such as the counter-rotating vortex pair (CRVP). Experimental data used for validation of the codes\ include mean axial velocity and jet fluid mixture fraction profiles (at three distinct axial locations), jet trajectory, turbulent kinetic energy distributions, and velocity and mixture fraction cross-plane distributions. All CFD results except CFD++, exhibit symmetrical solutions about the center plane. The current investigation shows that although all codes considered predict the experimental data with various degrees of accuracy, Fluent using the standard k-□ turbulence model with the standard ll function, and LES results compare exceptionally well with the experimental data for this flow regime and configuration.

15. SUBJECT TERMS

16. SECURITY CLASSIFICATION OF:			**17. LIMITATION OF ABSTRACT**	**18. NUMBER OF PAGES**	**19a. NAME OF RESPONSIBLE PERSON**
					Nils Sedano
a. REPORT	**b. ABSTRACT**	**c. THIS PAGE**			**19b. TELEPHONE NO** *(include area code)*
Unclassified	**Unclassified**	**Unclassified**	SAR	13	661-275-5972

Standard Form 298 (Rev. 8-98)
Prescribed by ANSI Std. 239.18

NUMERICAL SIMULATION OF CONFINED MULTIPLE TRANSVERSE JETS

Farhad Davoudzadeh[1]
U.S. Air Force Research Laboratory (AFRL), Edwards AFB, California 93524

David Forliti[2]
Jackson and Tull/*AFRL-RZSE*, Edwards AFB, CA, 93524

Anh-Tuan Le[3], Henry Vu[4]
Advatech Pacific, Inc. San Bernardino, California 92408 U.S.A.

ABSTRACT

Behavior of unconfined transverse jets has been studied extensively, but little work is reported on the flow characteristics of confined transverse jets. The latter has been numerically investigated using a number of RANS codes. The computational results obtained from these codes have been evaluated against the existing experimental data, and the results of a Large-Eddy Simulations (LES) code reported in the literature. Furthermore, an extensive validation effort has been conducted to characterize the performance of the codes for predicting the flow within a propulsion-related mixing configuration. The validation case involves eight circumferentially spaced transverse jets issuing radially into an axisymmetric main flow, a configuration relevant for gas turbine burners and new liquid rocket engine preburners. The main flow Reynolds number was 1.7 x 10^5 and the jet-to-main flow momentum flux ratio was sixteen. The momentum and scalar mixing was investigated through the solution of the Reynolds-Averaged Navier Stokes (RANS) equations. The solutions of three commercial RANS solvers, Fluent, STAR-CCM+, and CFD++, are compared to experimental data and large-eddy simulation (LES) results available in literature. Due to demonstrated periodicity, only a one-eighth pie-shaped section of the geometry was considered. The different commercial codes used the same geometry, grid, boundary conditions, and variations of the k-ϵ turbulence model. The LES results obtained from literature used a different grid, but the same geometry. All numerical simulations using the above mentioned codes capture salient flow structures such as the counter-rotating vortex pair (CRVP). Experimental data used for validation of the codes include mean axial velocity and jet fluid mixture fraction profiles (at three distinct axial locations), jet trajectory, turbulent kinetic energy distributions, and velocity and mixture fraction cross-plane distributions. All CFD results except CFD++, exhibit symmetrical solutions about the center plane. The current investigation shows that although all codes considered predict the experimental data with various degrees of accuracy, Fluent using the standard k-ϵ turbulence model with the standard wall function, and LES results compare exceptionally well with the experimental data for this flow regime and configuration.

---

[1] Senior Scientist, Air Force Research Laboratory, 4 Draco Drive, Edwards AFB, California
[2] Research Scientist, Jackson and Tull, AFRL/RZSE, 4 Draco Drive, Edwards AFB, California
[3] Staff Engineer, Advatech Pacific, Inc., 560E Hospitality Lane, San Bernardino, California 92408 U.S.A.
[4] Staff Engineer, Advatech Pacific, Inc., 560E Hospitality Lane, San Bernardino, California 92408 U.S.A.

Nomenclature

A, b, c	=	empirical constants
C	=	local mean mass fraction of the jet
$\overline{C}$	=	average mass fraction of the jet over the cross sectional area A
D	=	diameter
J	=	momentum flux ratio
$\dot{m}$	=	mass flow rate
n	=	number of jets
Q	=	volume flow rate
r	=	velocity ratio
x	=	streamwise coordinate
y	=	cross stream coordinate
$_j$	=	subscript for jet flow
Us	=	Unmixedness

I. Introduction

Transverse jets, or jets in cross flow (JICF), provide an effective mixing mechanism, via vortical structures, that can be utilized in a number of applications. Examples of these applications include mixing of diluents with core fluid in a liquid rocket engine preburner or gas turbine, vertical and short take-off and landing (V/STOL) aircraft, and film cooling of turbine blades. Past studies have demonstrated that excessive temperature variations at the turbine inlet have a detrimental effect on turbine life and performance. In staged combustion rocket engines, the function of a preburner is to provide combustion gases that will drive the turbine, which in turn drive the pumps, before being exhausted into the main combustion chamber. Survival and durability of the turbine blades depends upon thermal stresses applied by the combustion hot gases exhausted by the preburner. The cooler and the more uniform the combustion gases the better the survivability of the turbine blades. In this application the LOX diluent jet in the cross flow can provide enhanced mixing mechanism of the combustion gases to provide a uniform inlet to the turbine.

The rocket preburner offers a number of technical challenges for CFD, including turbulent combustion, complex geometry with strong streamline curvature, very large density ratio between the mixing fluids, and transcritical phenomena due to the high operating pressure. The current validation effort is essentially the first phase of an overarching process of validating codes for rocket preburners, and employs currently available experimental data associated with a gas turbine burner configuration [1, 2].The experimental setup involved an eight JICF configuration issuing into a fully-developed pipe flow with both fluids being air nominally at standard temperature and pressure. The purpose of this phase of the validation effort is to establish a foundational methodology that is able to accurately simulate the complex geometry in a preburner-like configuration. This will essentially establish a departure point as we incrementally add salient features of the preburner, including density ratio, high pressure, and chemistry.

The experimental work was numerically modeled using three different computational fluid dynamics (CFD) Codes: Fluent, CFD++, and STAR-CCM+. The computational work was performed to identify the current capabilities of the CFD tools in modeling the complex flow structures encountered in JICF, and to identify the appropriate CFD model elements (solver, turbulence model, computational extend and grid, etc.) related to the flow regime under consideration. Current simulations show a good comparison between the computational results obtained by Fluent and STAR-CCM+ and identifies relevant CFD parameters (turbulence model, geometry and grid distribution, solver type) of importance in this flow regime. Efforts are continuing to perform more detailed calculations looking into grid resolution, boundary conditions, and solver models.

Demuren [3] categorized four different models, in terms of accuracy, that has been used in investigations of the JICF: empirical, integral, perturbation and numerical. The empirical method is the simplest model that relies on the correlation of experimental data, and the accuracy of an empirical model will in general depend on whether a given point of interest lies within the cloud of data used for

construction of the correlation; the empirical model is essentially a curve fit. Due to their low cost and ease of use, empirical models are most useful for first-order estimates and as qualitative checks for results produced by other methods.

One of the the most common JICF attributes treated using empirical models is the jet trajectory. For a single circular turbulent jet injected normally into a cross flow, the trajectory has the form [3]:

$$\frac{y}{D} = aJ^{b}\left(\frac{x}{D}\right)^{c}$$

where D is the jet diameter, J is the momentum flux ratio, x and y are the cross-stream and streamwise coordinates of the jet trajectory, and a, b, and c are empirical constants. In the range of J between 2 and 2,000, a has a value between 0.7 and 1.3, b has a valuebetween 0.36 and 0.52 and c takes a value between 0.28 and 0.40, depending on experimental conditions [3].

On the other end of the spectrum, Demuren [3] pointed out that "numerical models have the most potential for wide generality and can, in principle, be applied to the whole range of jet in cross flow situations, confined or unconfined, low, medium or high J, single or multiple jets, impinging on a wall or on other jets, swirling, homogeneous or heterogeneous cross flow, compressible or incompressible, etc."

The research results presented in this paper numerically investigates the various flow characteristics experienced when jets and cross flow interact, and studies the induced resultant flow structures and their contribution to the mixing of the propellants. For validation and verification of the simulations, the numerical work uses several RANS codes and compares the simulation results against experimental data and a large-eddy simulation (LES) available in the literature.

II. Geometry and Grid

The experimental data used for validation of the computational work are obtained from the work performed by A. Strzelecki, et al. [2-3]. In these experiments, the mixing of eight isothermal jets issuing into a circular pipe flow is investigated by means of laser Doppler anemometry, particle image velocimetry, and planar laser-induced fluorescence techniques. The measured variables include velocity and scalar concentration fields. Approximation of the geometry, in the vicinity of the diluent injection ports, is shown in Figure 1.

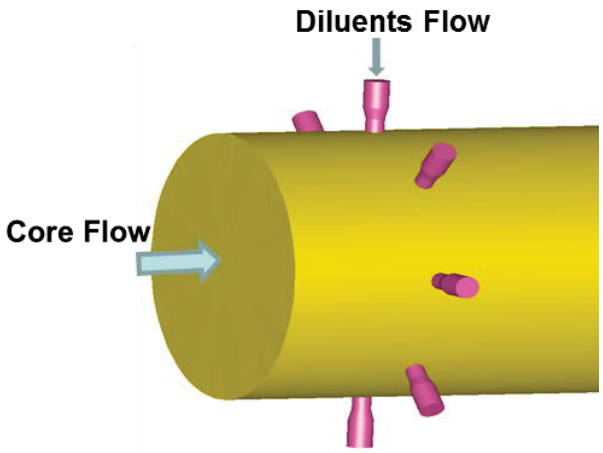

Figure 1. Geometry in the vicinity of the jet injection system.

It should be noted that this geometry is constructed for the CFD analysis and is considered to closely represent the experimental configuration. A similar simplification of the geometry is also adapted by the original investigators [3] for their LES calculations.

Figure 2, shows the grid distribution (a) on and around an injection port, and (b) at the inlet/exit of the core flow. A total of approximately 800k hexahedral only elements are used. As shown in the inlet/exit grid distribution, no singularity axis is used in the construction of the grid. Wall grid distribution corresponds to a y+ of 0.71 -1.2.

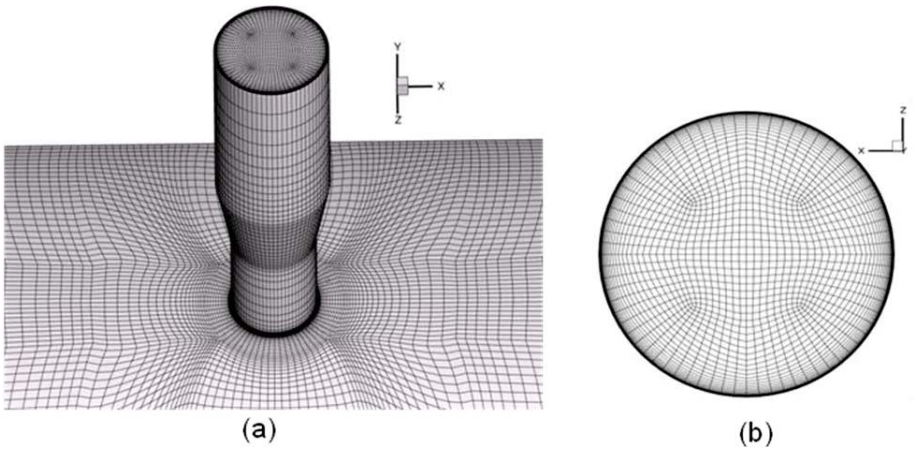

Figure 2. (a) Grid distribution on an injection port (b) and at the core-flow inlet/exit

III. Computational Domain and Boundary Conditions

Figure 3 shows the computational domain and the boundary conditions used in the simulation. To take advantage of symmetry in the geometry, only a forty-five degree pie section of the geometry is simulated, with the planes of symmetry specified at each side of the pie, as shown in the figure. The upstream boundary is located 10D upstream of the diluent injection port, where D is the main pipe diameter. The downstream boundary condition is similarly located 10D downstream of the injection port. The upstream BC is specified at an inlet velocity of 25 m/s. The inlet jet velocity is 58.1 m/s. Considering the contraction of the jet tube before intersection with the main pipe, the jet velocity at the jet orifice is 100 m/s. This dictates a velocity ratio (jet to main flow) to be (100/25=) 4, that corresponds to a momentum flux ratio of 16. The exit BC uses the static pressure and is set to standard atmospheric pressure. The main core diameter is 100 mm, the jet diameter is 8.1 mm that contracts to 6.1 mm at the orifice. These conditions match that for the experimental and LES data. The fluid used for both diluent inlet and for the main core flow is air.

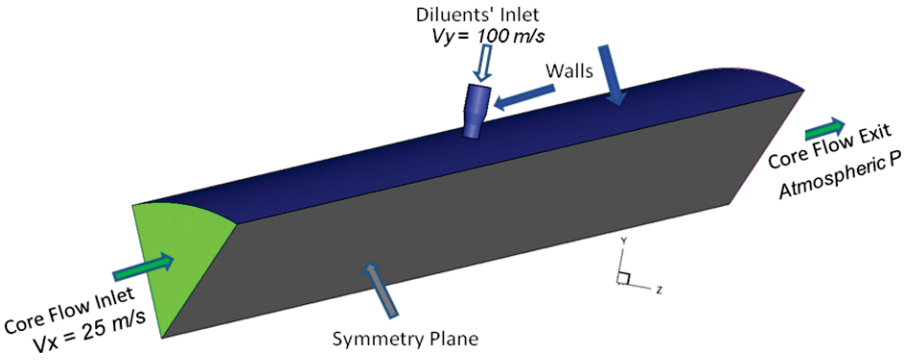

Figure 3. Computational domain and boundary conditions.

IV. Flow Solver and Operating Conditions

All simulations are 3D, second-order accurate, using Ansys-Fluent (pressure-velocity coupled) flow solver Release 13.0., CFD++ version 10.1.1, and STAR-CCM+ version 6.02.007. In addition, the LES results from Priere et al. [2] are also considered. Equations solved are x-, y-, and z-momentum, energy, turbulent kinetic energy (TKE), turbulent dissipation rate (TDR), species mass fraction, and continuity. The second-order spatial discretization solution method was used in all calculations.

The inlet boundary conditions (BC) specify velocity, temperature, and turbulence intensity. The exit BC sets static pressure and temperature. Walls are no slip and adiabatic. Turbulence models considered include the standard and realizable two equation k-ϵ models using standard, enhanced, or the low Reynolds number wall treatment options.

All the results presented are after the numerical iteration has converged. Convergence is considered achieved when the residuals of the equations being solved have dropped by approximately four orders of magnitude, the residual gradients have approached zero and have plateaued, there are negligible changes in the flow variables, and mass is conserved throughout the computational domain. All calculations are performed on a four processor workstation. Simulations using Fluent typically took approximately 10000 iterations to achieve a fully-converged solution. This typically took about 24 hours, dependent on how many grid points were used. On the quad-core Intel Zeon processor the clock time used was 25 x 10-3 microseconds per iteration per grid point.

V. Computational Results and Experimental Data

FLOW CHARACTERISTICS:

Flow characteristics of the JICF are described in detail by Fric & Roshko [4]. The flow is dominated essentially by four different types of vortical structures as shown in figure 4:

(1) A counter rotating vortex pair (CRVP). This vortex pair is the most dominant flow feature in the JICF. It is generated by the realignment of jet shear layer vorticity through a complex interaction with the cross flow [5]. The CRVP is the primary flow structure responsible for mixing of the jet and the core flow.

(2) Horseshoe vortex: generated at the root of the jet as it enters the cross flow. This type of vortex structures is a typical flow pattern that is created around a bluff body mounted normal to a surface. It is generated due to the adverse pressure gradient on the windward side of the jet and the adjacent wall due to the dynamic pressure profile within the boundary layer.

(3) Jet shear layer vortices: these vortices originate from instability of the separated boundary layer at the orifice of the jet and evolve around the surface of the jet. The shearing of the core flow via the jet flow generates Kelvin-Helmholtz instability causing the flow, in the shear region, to roll up to a ring vortex around the jet.

(4) Wake vortices: these vortices are found in the wake of the jet and they connect the CRVP to the wall. These structures where initially investigated experimentally by Fric and Roshko [4].

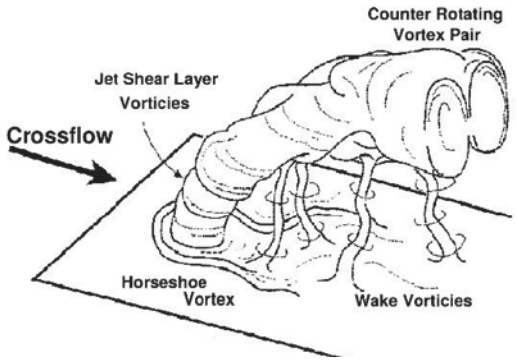

Figure 4. Schematic of various vortex structures in JICF, adapted from Fric & Roshko [3]

The RANS numerical simulation using ANSYS-Fluent captured some of these vortical structures as described in the following. Figure 5 shows an isometric view of the flow field. The characteristic velocity Uo is the mean velocity at the main pipe inlet. The non-dimensional axial velocity gives an indication of the extent of the jet. The figure also shows three-dimensional streamlines in the cross-sectional planes normal to the axial direction. These streamlines delineate the CRVP. Expansion of the CRVP in the axial direction is demonstrated in these cross-sectional streamlines.

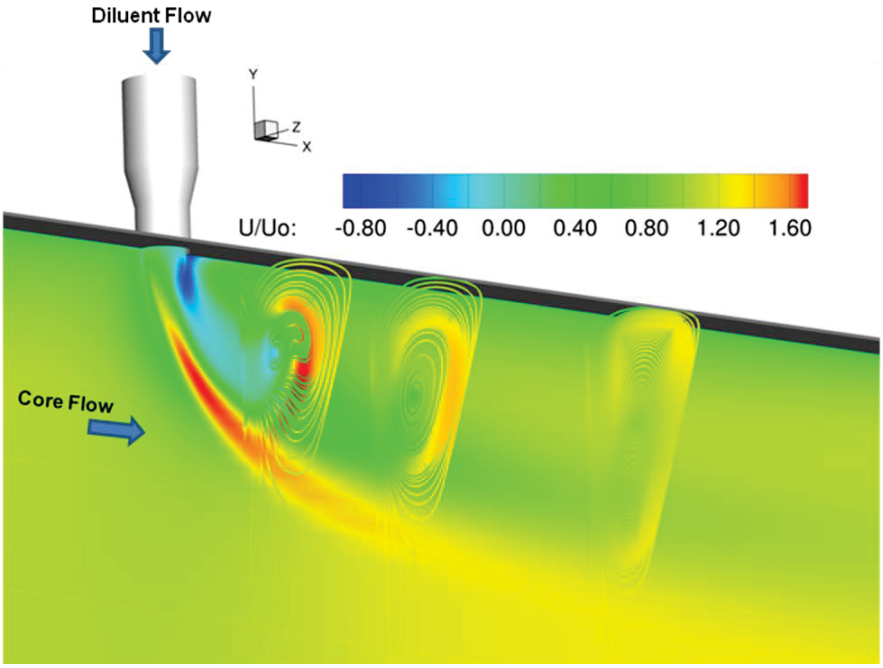

Figure 5. Axial velocity & cross sections including streamlines showing CRVPs' structure (ANSYS-Fluent simulation)

VELOCITY DISTRIBUTION:

Figure 6 shows contours of streamwise velocity at axial cross sections 2d, 5d, and 10d (d is the diameter of the jet) downstream of the jet for the computational results obtained using Fluent, STAR-CCM+, CFD++, LES, and the experimental data. Comparing the velocity distributions, it is evident that LES and Fluent results compare very well with the experimental data for all the axial locations considered. The RANS simulations shown in the figure were run using the standard k-ϵ model turbulence model with standard wall function, except CFD++ where the standard k-ϵ model was not available and the realizable k-ϵ model with the wall function was used. A noticeable feature in the CFD++ results is the asymmetry in the solution that becomes very pronounced at the axial station of x = 10d. This was brought to the attention of Metacomp Technologies, the developers of the CFD++ software, in a private communication. Consequently, Metacomp ran a calculation in which they indicated that "in order to obtain a non-oscillating steady-state solution, flux blending was used with 75% second-order flux blended with 25% first-order flux". Metacomp also indicated that when run in higher-order transient mode, this type of flow configuration has a tendency to develop asymmetries which should be expected to change the time-averaged interior flow-field, including the exit mass fluxes.

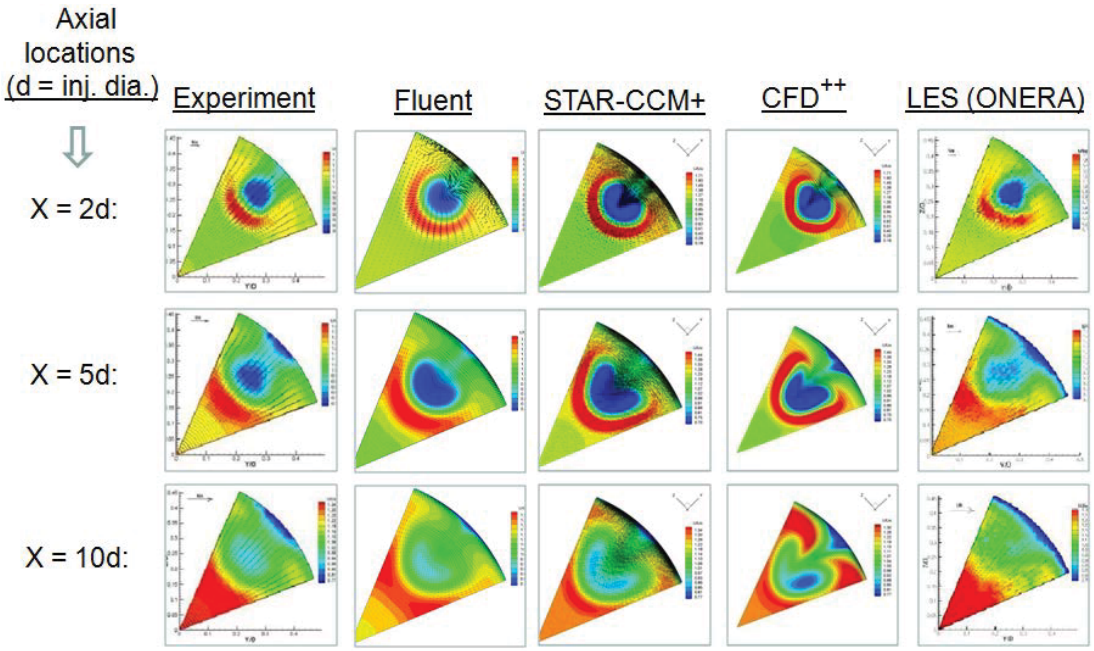

Figure 6. Axial velocity distribution at different axial stations

Figure 7 compares computational radial profiles of axial velocity, obtained via the above mentioned codes, with the experimental data at axial locations of x = 2d, 5d, and 10d downstream of the injection port, where d is the jet orifice diameter. At the axial station of x = 2d, all codes predict the experimental profiles of the axial velocity very well, but for the locations of x = 5d, and x = 10d the LES and the Fluent predictions are much closer to the experimental data than CFD++ and STAR-CCM+.

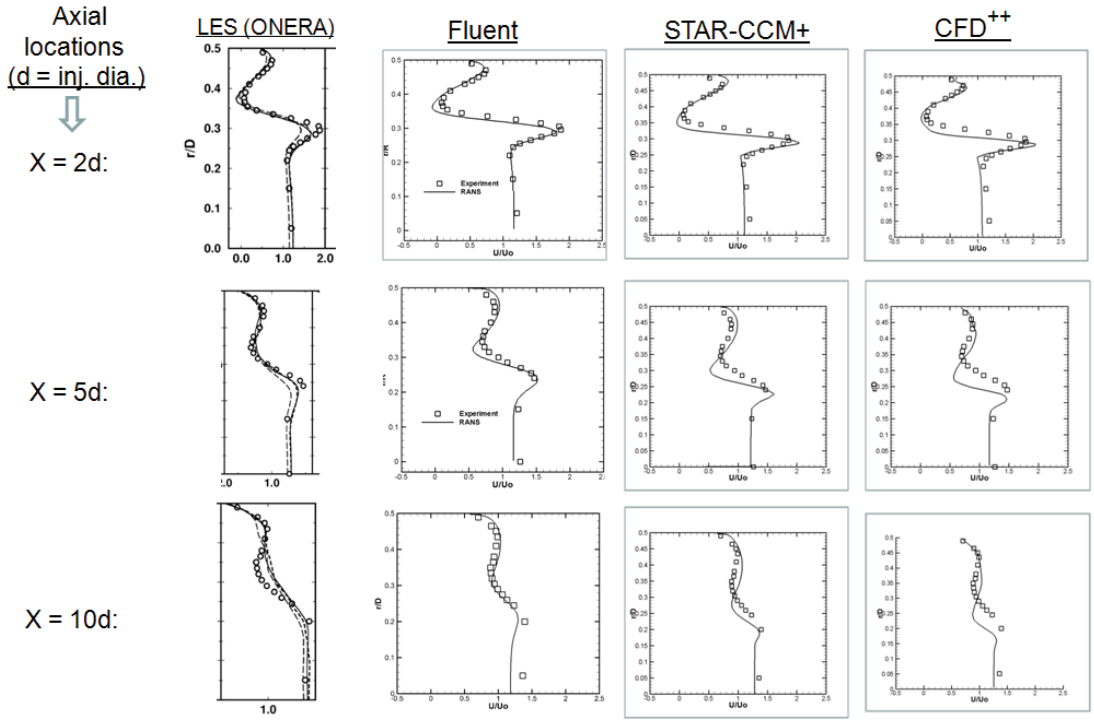

Figure 7. Predicted vs. experimental radial profiles of the axial velocity at different axial locations

Figure 8 shows comparison of the experimental data with the Fluent predictions using the standard k-ϵ and the realizable k-ϵ models, and the CFD++ predictions using the realizable k-ϵ model. The figure demonstrates that the Fluent and the CFD++ predictions show similar patterns when the realizable k-ϵ model is used. This could be attributable to the turbulence models constants used in the standard k-ϵ and the realizable k-ϵ models. The standard k-ϵ models uses five constants, namely $C\mu = 0.09$, $C1\epsilon = 1.44$, $C2\epsilon = 1.92$, $\sigma k = 1.0$, and $\sigma\epsilon = 1.3$ whereas in the realizable k-ϵ model $C1\epsilon$ and $C\mu$ are not constants [6]. In particular, the maximum value that can be allowed in the realizable k-ϵ model for $C\mu$, in the whole computational domain, is 0.09. In most cells this value is smaller than 0.09. Considering the transport equations for the k-ϵ turbulence model, the higher value of the $C\mu$ would lead to a higher production of the turbulent kinetic energy when the standard k-ϵ is used versus the realizable k-ϵ (see Figure 9), and this may be responsible for the better predictions when the standard k-ϵ model is used.

Similar conclusions were observed by Karvinen et al [7], and by Menzies [8]. Karvinen et al conducted numerical simulation on a circular jet in a cross flow using Fluent employing various turbulence models and concluded that results from standard k-ϵ model were closest to the measured values. The turbulence models that were evaluated by him included three high-Reynolds number k-ϵ models, two k-ω models, six low-Reynolds number k-ϵ models as well as the Reynolds stress model. Menzies [8] also evaluated various turbulence models for a similar flow regime for the isothermal flow in a gas turbine combustion system and concluded that of the turbulence models used, the realizable model performed poorly, while the renormalization group (RNG) method did not deliver any benefits to the velocity predictions, but the standard k-ϵ model delivered acceptable results in comparison with the measurements.

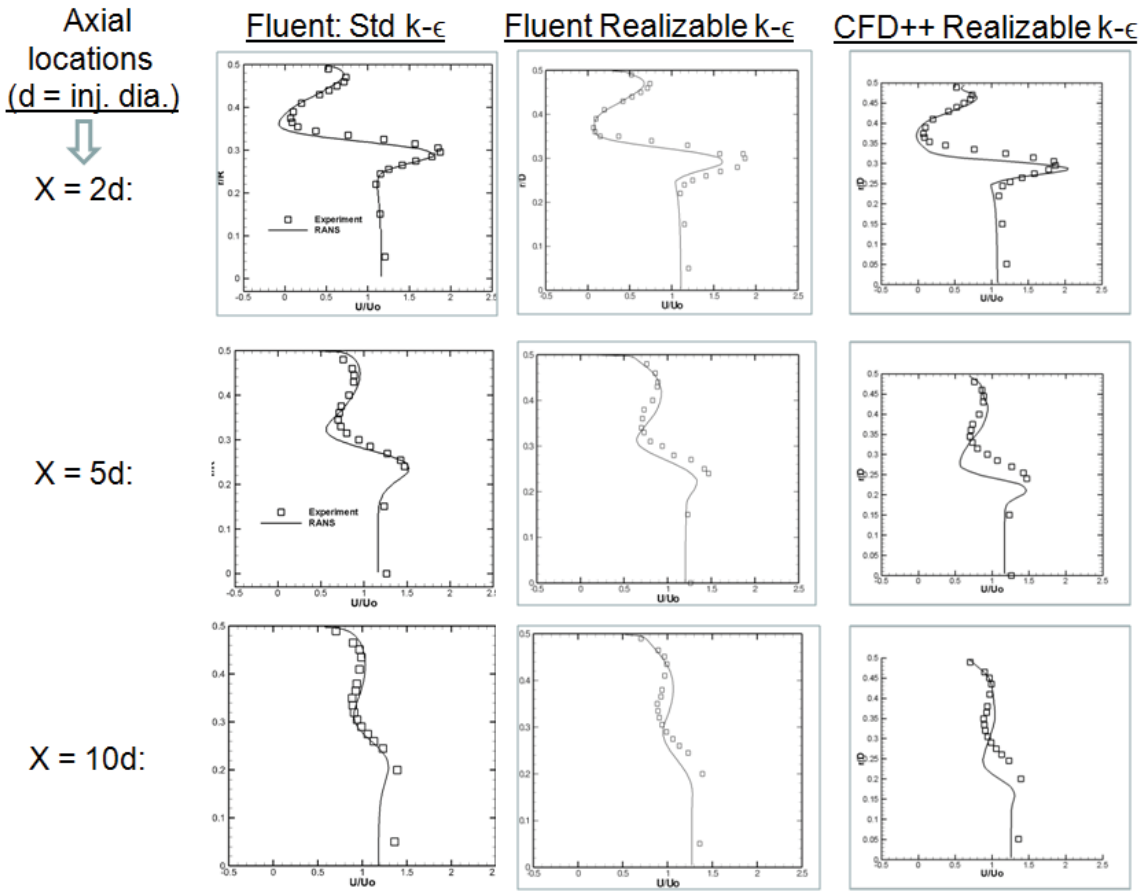

Figure 8. Experimental data vs. predicted radial profiles of the axial velocity using standard k-ϵ and realizable k-ϵ

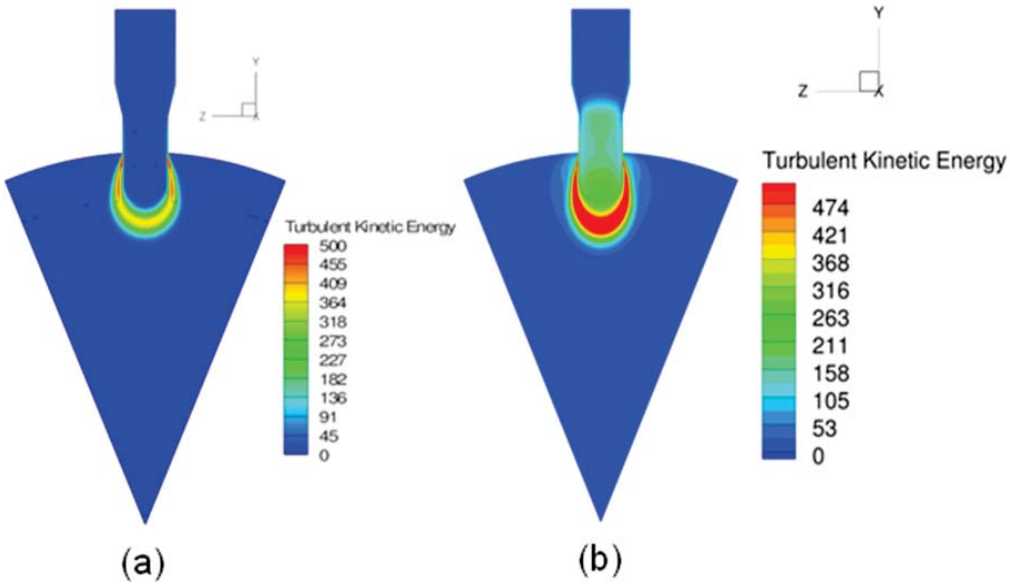

Figure 9. Predicted turbulent kinetic energy with Fluent (a) Realizable k-ϵ with enhanced wall treatment (b) Standard k-ϵ with standard wall function

There is a disagreement between a significant number of authors about two-equation turbulence models and their application for different flow regimes. As Menter [9] has pointed out, "there is no agreement on the standards by which to measure the improvements achieved by proposed new models, or alterations to the existing models. Many times new models are based on theoretical concepts, which by themselves involve severe assumptions about the nature of turbulence. It is often unclear whether the improvements presented for one type of flow (e.g., boundary-layer flows) will not lead to deterioration for another class of equally important flows (e.g., free shear flows)." For example, an argument had been made by Pope [10] in 1978 that the standard k-ϵ model overestimates spreading of the round jet and suggested corrections to the model. However, as pointed out by Rubel [11], the Pope correction has an adverse effect on the model predictions for the radial jet and underestimates the radial jet spreading by 60%.

Again as Menter [9] has stated "none of the available theoretical tools (dimensional analysis, asymptotic expansion theory, use of direct numerical simulations (DNS) data, renormalization group (RNG) theory, rapid distortion theory, etc.) can provide constants to that degree of accuracy. The only way to establish the validity of theoretical arguments is to carefully test the resulting model against a number of challenging and well-documented research flows." The comparison with the experimental data is usually believed to allow some conclusions about a model's ability to perform in engineering applications.

SCALAR CONCENTRATIONS:

Figure 10 shows the jet species mass fraction distribution at the longitudinal cross section for the experimental data and the computational codes considered. The experimental data shows a more rapid expansion of the jet scalar field than STAR-CCM+ and CFD++. Fluent results again show a better matching with the experimental data than the other two codes.

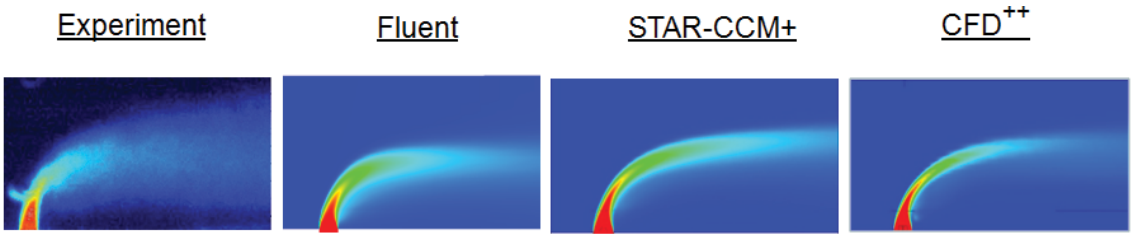

Figure 10. Jet mass fraction distribution

Experimental and predicted concentration radial profiles at the axial locations of x = 2d, 5d, and 10d are shown in Figure 11 and similarly shows that the Fluent results are in much better agreement with the experimental data than STAR-CCM+ or CFD++.

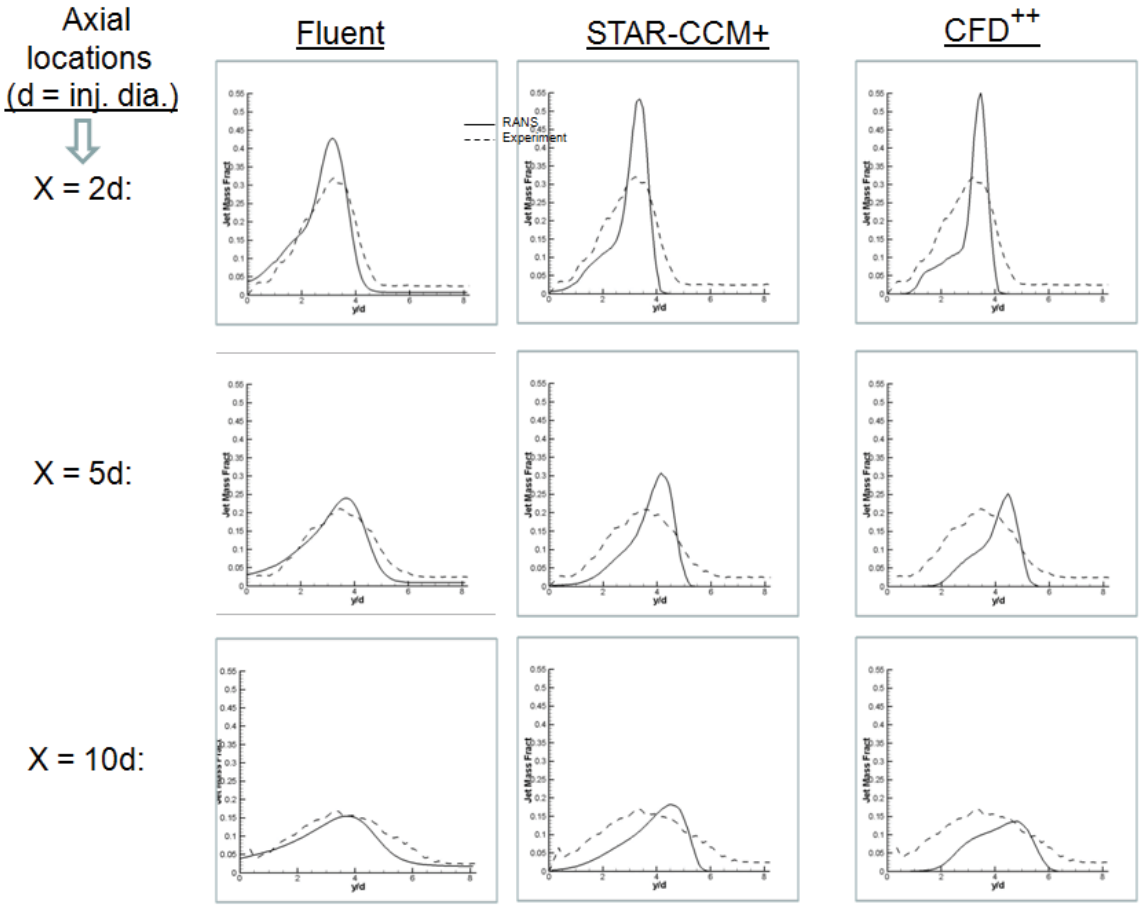

Figure 11. Computational and experimental jet concentration profiles at x = 2d, 5d, and 10d

Figure 12 shows the degree of mixing of the jet flow with the core flow. The unmixedness parameter Us is defined as:

$$U_s = \frac{\sigma_C^2}{\overline{C}\left(1-\overline{C}\right)} = \frac{\frac{1}{A}\int \left(C-\overline{C}\right)^2 dA}{\overline{C}\left(1-\overline{C}\right)},$$

where σ_C is the statistical variance of the jet's mass fraction in the cross plane at a given axial location (X/d), C is the local mean mass fraction of the jet, and $\overline{C}$ is the average mass fraction of the jet over the cross sectional area A.

Consistent with the contour plots of the jet mass fraction shown in Figure 10, Fluent results show a higher degree of mixedness than the other codes.

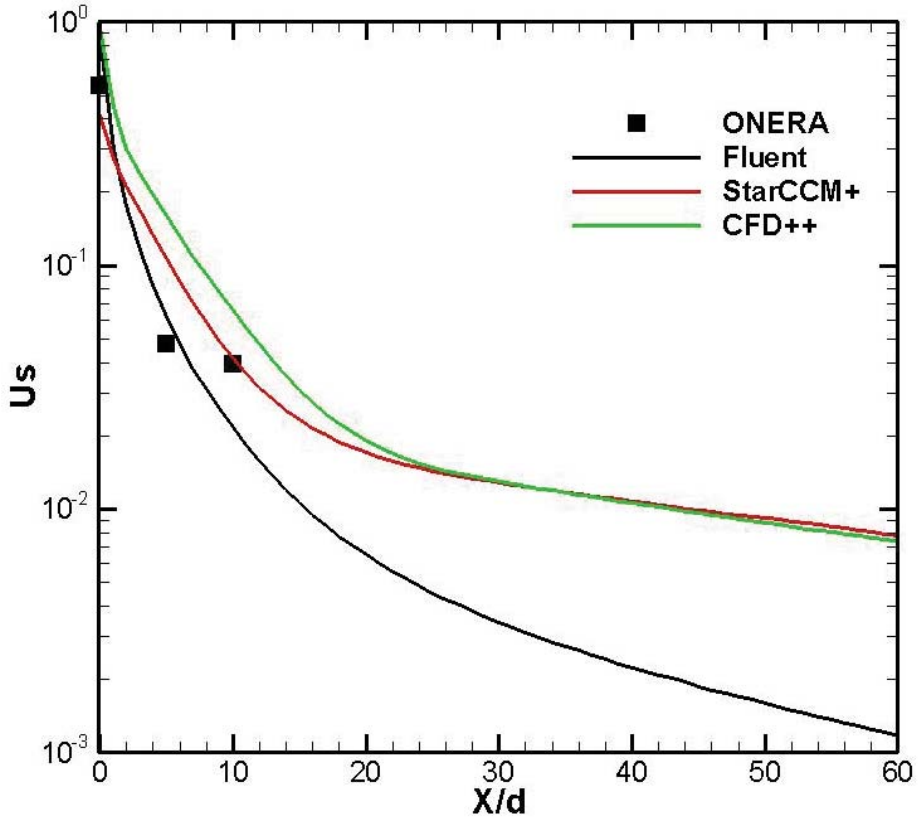

Figure 12. Experimental and predicted unmixedness

VI. Conclusions

A series of numerical simulations is performed to predict the flow induced by eight isothermal jets issuing in a circular pipe flow. The computational codes used for these simulations included an LES code, Fluent, STAR-CCM+, and CFD++ codes. The computational parameters were chosen to be identical for

the codes under consideration, noting that some limitations were present in the options for the different codes. The turbulence model used in these simulations was the standard k-ϵ model with the standard wall function for Fluent and STAR-CCM+, and the realizable k-ϵ model with the standard wall function for the CFD++; standard k-ϵ is not available in the CFD++ code. Further, the computational results were compared with the experimental data for the velocity distributions, concentration distributions, velocity profiles, and scalar concentration radial profiles at various axial stations.

All simulations captured the dominant counter rotating vortex pair (CRVP) flow structure, known to be present in the JICF flow regime. Quantitative comparison of the experimental data with the computational results for the radial profiles of the axial velocity and the jet concentration showed that Fluent, using the standard k-ϵ, predictions were closer to the experimental data than either STAR-CCM+ or CFD++. This conclusion is consistent with similar conclusions reported in the literature [7, 8].

References

1. Strzelecki, A., et. al..: "Experimental Investigation of the Jets in Crossflow: Nonswirling Flow Case," AIAA Journal, Vol. 47, No.5, May 2009.

2. Priere, C., et. al.: "Experimental and Numerical Studies of Dilution Systems for Low-Emission Combustors," AIAA Journal, Vol. 43, No.8, August 2005.

3. Demuren, A. O., "Fundamentals of fluid mechanics: Modeling Turbulent Jets in Crossflow," Edited by: Schetz, J. A., Fuhs, A. E. pp. 797 John Wiley & Sons, 1999

4. Fric, T. F. & Roshko, A. 1994 Vortical structure in the wake of a transverse jet. J. Fluid Mech. 279, 1–47.

5. Cortelezzi, L, and Karagozian, A.R., "on the formation of the counter-rotating vortex pair in transverse jets," JFM, V. 446, n. 1, pp. 347-373, 2001

6. Shih T.-H., Liou W. W., Shabir A., Yang Z., and Zhu, J (1995). "A new k-ϵ eddy viscosity model for high Reynolds number turbulent flows," Computers and Fluids 24, pp 227-238.

7. Karvinen, A. and Ahlstedt, H.: "Comparison of turbulence models in case of jet in crossflow using commercial CFD code," Engineering Turbulence Modeling and Experiments 6, pp-399. Proceedings of the ERCOFTAC International Symposium on Engineering Turbulence Modeling and Measurements – ETMM6 – Sardinia, Italy, 23-25 May, 2005.

8. Menzies, K. R.:"An evaluation of turbulence models for the isothermal flow in a gas turbine combustion system," Engineering Turbulence Modeling and Experiments 6, pp-741. Proceedings of the ERCOFTAC International Symposium on Engineering Turbulence Modeling and Measurements – ETMM6 – Sardinia, Italy, 23-25 May, 2005.

9. Menter, F. R., "Two-equation eddy-viscosity turbulence models for engineering applications," AIAA Journal 1994, vol.32 no.8

10. Pope, S. B. "An explanation of the turbulent round-jet/plane-jet anomaly," Technical Notes, AIAA, Vol. 16, NO. 3, pp-279, 1978

11. Rubel, A. "On vortex stretching modification of the k-ϵ turbulence model: radial jets," AIAA Journal, Vol. 23, No. 7, pp. 1129-1130